Shape Effects of Cu 2 O Polyhedral Microcrystals on Photocatalytic Activity

ARTICLE *in* THE JOURNAL OF PHYSICAL CHEMISTRY C · MARCH 2010

Impact Factor: 4.77 · DOI: 10.1021/jp9110037

5 AUTHORS, INCLUDING:

Tierui Zhang
Technical Institute of Physics and Chemistry
109 PUBLICATIONS **3,158** CITATIONS

SEE PROFILE

Shape Effects of Cu_2O Polyhedral Microcrystals on Photocatalytic Activity

Ying Zhang,[†] Bin Deng,[†] Tierui Zhang,*[,‡] Daming Gao,[§] and An-Wu Xu*[,†]

Division of Nanomaterials and Chemistry, Hefei National Laboratory for Physical Sciences at Microscale, University of Science and Technology of China, Hefei 230026, China, Key Laboratory of Photochemical Conversion and Optoelectronic Materials, Technical Institute of Physics and Chemistry, Chinese Academy of Sciences, Beijng 100190, China, and Department of Chemistry and Materials Engineering, Hefei University, Hefei 230026, China

Received: November 19, 2009; Revised Manuscript Received: February 8, 2010

Perfect mixed 26-facet and 18-facet polyhedra of Cu_2O microcrystals were successfully synthesized by a hydrothermal process with use of stearic acid as a structure-directing agent. Cu_2O octahedra and cubes were also prepared under hydrothermal conditions. The obtained microstructures were characterized by X-ray diffraction (XRD), transmission electron microscopy (TEM), high-resolution TEM (HRTEM), and UV−vis spectrum. The adsorption and photocatalytic activity of as-prepared 26-facet and 18-facet Cu_2O polyhedra for decomposition of methyl orange were investigated and compared to that of octahedra and cubes. The results show that mixed 26-facet and 18-facet polyhedra with dominant {110} facets have a higher adsorption and photocatalytic activity than Cu_2O octahedra with dominant {111} surfaces and cubes with {100} surfaces. A higher surface energy and a greater density of the "Cu" dangling bonds on {110} facets of 26-facet and 18-facet polyhedra may be ascribed to its higher catalytic activity. Moreover, as compared with octahedra and cubes, mixed 26-facet and 18-facet polyhedra have more edges and corners, which could improve photocatalytic activity. This simple one-pot synthetic route could provide a good starting point for the research of morphology construction and shape-dependent catalytic properties of other materials.

Introduction

As the way that a crystal is organized and structured will determine the behavior of the atoms that constitute the crystal, catalytic activity depends on the surface structure of a crystal with high activity. In a recent El-Sayed and Narayanan's work, catalytic activity of Pt nanocrystals was correlated with their surface atoms.[1] It has been demonstrated that the performance of catalysts can be enhanced by shape control as shape determines the number of atoms located at the edges, corners, or surfaces.[2,3] Polyhedra with highly reactive surfaces exhibit much higher catalytic activity than the common ones. For example, it has been reported that synthesized anatase TiO_2 nanosheets having dominant {001} facets (64%) display superior photoreactivity (more than 5 times) compared to P25 as a benchmarking material.[4] Unconventional polyhedron with high-index facets have a greater density of unsaturated atomic steps, ledges, and kinks that can serve as active sites for breaking chemical bonds than conventional polyhedron with low-index facets such as octahedron, cube, tetrahedron, and so on.[1,2,5] Tetrahexahedral (THH) platinum nanocrystals enclosed by {730}, {210}, and/or {520} facets fabricated by Sun and co-workers exhibit higher catalytic activity two to four times that of commercial platinum.[5] However, it is much more difficult to obtain the unconventional polyhedron because surfaces with high reactivity usually diminish rapidly during the crystal growth process as a result of the minimization of surface energy.

Up to now, numerous polyhedral materials have been synthesized such as noble metal polyhedra,[6] In_2O_3 octahedra, and SnO_2 octahedra,[7] and 18-facet Cu_7S_4 polyhedra with a hollow nanocage.[8] Cuprous oxide (Cu_2O), a p-type semiconductor with a direct band gap of about 2.17 eV, has potential applications in solar energy conversion, catalysis, lithium ion batteries, gas sensors, and electronics.[9] It crystallizes in a cuprite structure. During the past decade, some studies have been reported with regards to shape-controlled synthesis of Cu_2O micro- and nanocrystals such as nanowires,[10] multipods,[11] nanocubes,[12] octahedra,[13] and cuboctahedra.[14] Although Cu_2O crystals with various morphologies have been successfully synthesized, there are few papers that have reported on the preparation of 26-facet and 18-facet Cu_2O polyhedra with dominant {110} surfaces and their catalytic properties.[12–14]

Preferential adsorption of organic additives on certain crystallographic surfaces offers a good opportunity to tune and control the surface activities of materials. The rare occurrence of O−Cu−O 180° linear co-ordination of Cu_2O makes its crystalline facets of {111}, {100}, and {110} possess very distinctive chemical activities. It has been previously found that Cu_2O octahedra show better photocatalytic activity than cubes, because the {111} facets are more active than {100} facets due to the dangling bonds of {111} surfaces, while {100} facets have saturated chemical bonds and no dangling bands exist.[15,16]

In this work, perfectly mixed 26-facet and 18-facet polyhedra of cuprous oxide were synthesized by a simple hydrothermal method with use of stearic acid as a growth-directing agent. Both 26-facet and 18-facet Cu_2O polyhedra were found to display higher activity in the adsorption and photocatalytic decomposition of methyl orange than Cu_2O octahedra and cubes. To the best of our knowledge, this is the first experimental example where 26-facet and 18-facet Cu_2O polyhedra with

* To whom correspondence should be addressed. A. W. Xu. Phone: 86-551-3602346 (A.W.-W.). Fax: 86-551-3600724 (A.W.-W.). E-mail: anwuxu@ustc.edu.cn (A.W.-W.) and tierui@mail.ipc.ac.cn (T.R.Z.).
[†] University of Science and Technology of China.
[‡] Chinese Academy of Sciences.
[§] Hefei University.

10.1021/jp9110037
Published on Web 02/25/2010

dominant {110} facets have been obtained and the {110} facets of as-prepared Cu_2O polyhedra have higher photocatalytic activity than other surfaces such as {111} and {100} surfaces.

Experimental Section

All of the chemical reagents used in the experiments were of analytical grade and were used without further purification. In a typical synthesis of mixed 26-facet and 18-facet Cu_2O polyhedra, 1 mmol of $Cu(NO_3)_2 \cdot 3H_2O$ was dissolved in 5 mL of water and 10 mL of ethanol, and then 1 mmol of stearic acid (SA) were added into the above solution. After being sonicated in water for 10 min, the reaction was carried out in a Teflon-lined stainless steel autoclave at 180 °C for 12 h. The obtained solid was washed and filtered with ethanol and water several times and finally dried in air at 60 °C. For the synthesis of Cu_2O octahedra, 2 mmol of $Cu(NO_3)_2 \cdot 3H_2O$ was used while other reaction conditions were kept constant.

For the synthesis of Cu_2O cubes, 2.5 mL of formic acid was added to 37.5 mL of copper nitrate solution (0.02 M, the volume ratio of $C_2H_5OH:H_2O = 95:5$). After sonicated for 10 min, the solution was heated to 150 °C and kept for 2 h under hydrothermal conditions. The obtained product was washed several times and dried in air at 60 °C.

The X-ray powder diffraction (XRD) patterns of the samples were performed on a Rigaku/Max-3A X-ray diffractometer with Cu Kα radiation ($\lambda = 1.54178$ Å), the operation voltage and current maintained at 40 kV and 40 mA, respectively. Field emission scanning electron microscopic (FE-SEM) images were obtained with a JEOL JSM-6330F operated at a beam energy of 15.0 kV. Transmission electron microscopic (TEM) images, high-resolution transmission electron microscopic (HRTEM) images, and the selected area electron diffraction (SAED) patterns were performed on a JEOL-2010 microscope with an accelerating voltage of 200 kV. A Shimadzu spectrophotometer (Model 2501 PC) was used to record the UV−vis diffuse reflectance spectra of the samples.

The adsorption and photocatalytic activities for the different shaped Cu_2O microcrystals were investigated with use of methyl orange ($C_{14}H_{14}N_3NaO_3S$, MO) as a pollutant. Briefly, 0.05 g of Cu_2O samples was dispersed in 100 mL of methyl orange solution (15 mg/L). Before illumination, the solution was vigorously stirred in the dark for 5 h to evaluate the adsorption property. The photodegradation process was carried out at room temperature in a reactor of double layer condensated by running water to keep the temperature unchanged. Solution was irradiated by a 500 W xenon lamp equipped with a filter cutoff ($\lambda \geq 400$ nm). The MO concentration was analyzed by UV−vis absorption spectra, using a UV1800PC spectrophotometer.

Results and Discussion

The phase and purity of the as-obtained products were determined by X-ray diffraction (XRD) measurements. Figure 1 shows XRD patterns of as-prepared Cu_2O polyhedra in the presence of stearic acid by hydrothermal treatment and standard card of cuprous oxide cubic phase (JCPDS No. 05-0667). All of the peaks of the XRD pattern can be readily indexed to a pure cubic phase of Cu_2O with a lattice constant $a = 4.27$ Å. No other impurities were found in the samples. The intensity of the (220) peak is stronger than that of the (200) peak, which is different from the bulk cubic Cu_2O (JCPDS No. 05-0667), indicating a high proportion of {110} facets for the obtained 26-facet and 18-facet polyhedra.

The morphology and microstructure of 26-facet and 18-facet polyhedral products were examined by FE-SEM. A large

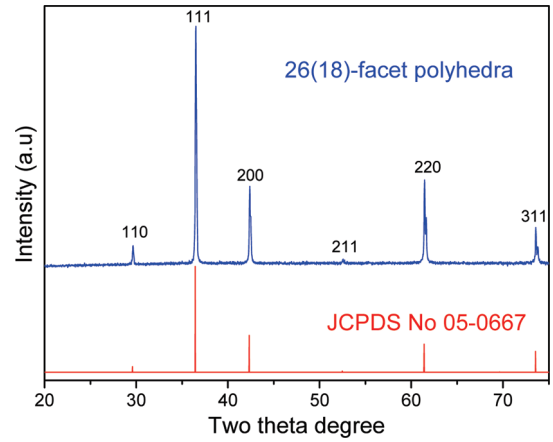

Figure 1. XRD pattern of the obtained Cu_2O 26(18)-facet polyhedra in the presence of stearic acid by hydrothermal treatment at 180 °C for 12 h.

number of polyhedral particles with an average size of 2 μm can be seen in the SEM image, as shown in Figure 2, parts a and b. A close examination of the sample clearly reveals that the sample consists of two kinds of morphologies. One is 18-facet polyhedron (Figure 2c), the other is 26-facet polyhedron (Figure 2d). The content of 26-facet polyhedra is about two-thirds and that of 18-facet polyhedra is about one-third in the final product (this mixed polyhedron is denoted 26(18)-facet polyhedron in the following text). The yield of the 26(18)-facet polyhedron is about 90%. It should be noted that we did not obtain pure 18-facet polyhedra or 26-facet polyhedra by changing the experimental conditions.

As shown in a model of an 18-facet polyhedron in Figure 3 (left), the exposed surfaces of the 18-facet polyhedron are made of 6 squares of {100} facets and 12 hexagons of {110} facets. There are 48 edges, 32 vertices in this 18-facet polyhedron. Among the 48 edges, 24 edges with a larger length form 6 square facets. The remaining 24 edges are shorter in length forming 8 vertices which are the joints with the 3 neighboring hexagons. In an 18-facet polyhedron, two types of vertices exist, one is the joint of three hexagons, and the other is the joint of two hexagons and one square. So this kind of 18-facet polyhedron is not an Archimedean polyhedron (vertices are identical).[8] A model of a 26-facet polehedron is shown in Figure 3 (right), which possesses 6 quadrangles of {100} facets, 12 {110} facets, and 8 triangles of {111} facets. There are 48 edges, 24 vertices in this 26-facet polyhedron. The 26-facet polyhedron structure can also be viewed as a result of cutting its 8 vertices of an 18-facet polyhedron. The 26-facet polyhedron belongs to one of 13 Archimedean solids, including only one type of vertex: the joint of three quadrangles and one triangle. From the SEM image of the 26-facet polyhedron in Figure 2d, it can be clearly seen that the edge length of {111} surfaces is shorter or equal to that of {100} surfaces, which makes the {110} facets rectangles or squares. The two types are in fact edge-cut cubes, not a Platonic polyhedron (one type of face).[17] Obviously, the number of edges and vertices of 26(18)-facet polyhedron are much more than those of cube and octahedron.

In the current synthetic system, SA serves as both a growth-directing reagent and reductant. Usually, organic acid can act not only as an acid, but also as a reducing agent, a facility that has been widely investigated in previous work.[18] In the face-centered cubic lattice, the relative surface energies are in the order of $\gamma_{\{111\}} < \gamma_{\{100\}} < \gamma_{\{110\}}$ among the lowest index planes, due to the surface-atom density and coordination number with

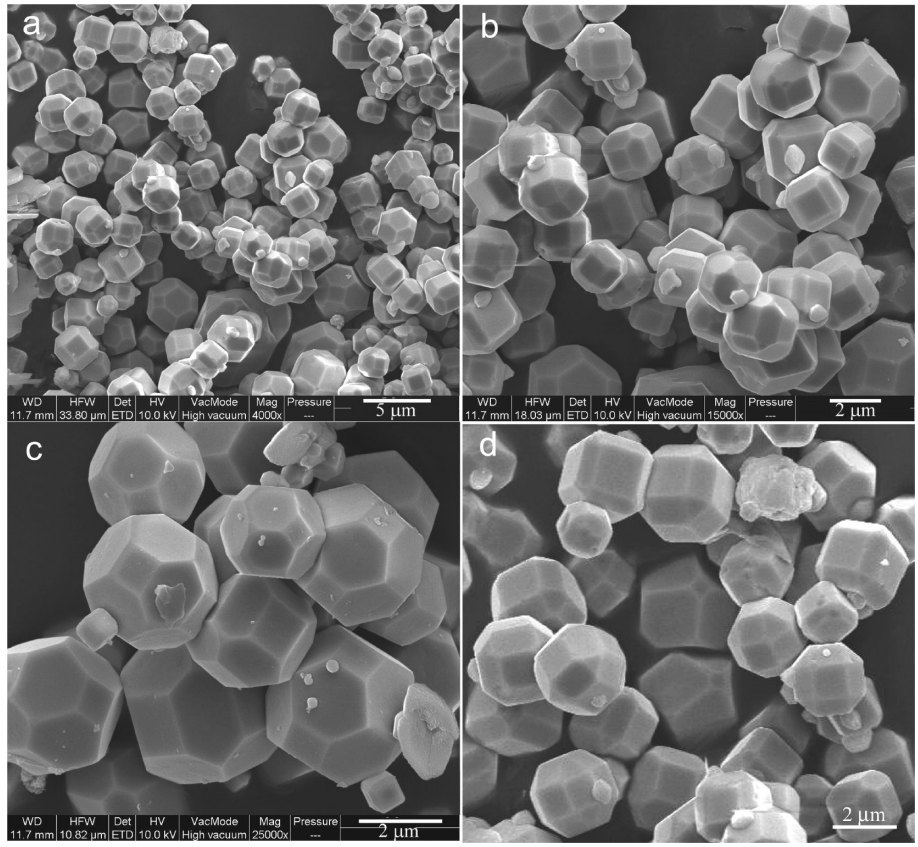

Figure 2. SEM images of the as-made Cu_2O 26(18)-facet polyhedral crystals (a, b) grown in the presence of stearic acid by hydrothermal treatment at 180 °C for 12 h; (c) the enlarged SEM image of 18-facet polyhedra; and (d) the enlarged SEM image of 26-facet polyhedra.

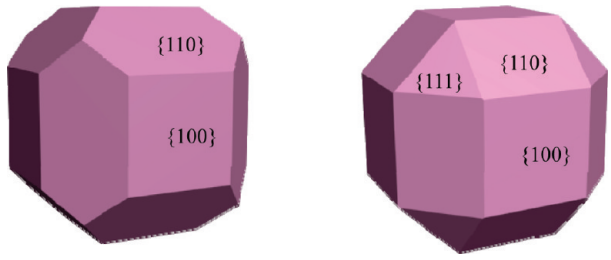

Figure 3. Three-dimensional view of an 18-facet polyhedral model (left) and a 26-facet polyhedral model (right).

neighboring atoms.[19] To minimize the total surface energy, the introduced SA molecules would prefer to adsorb onto the higher energy surfaces {110} during the crystal growth. The adsorption stabilizes the {110} facets and thus hinders the growth rate perpendicular to it. This leads to the exposure of the large {110} surfaces and the formation of the final 26(18)-facet Cu_2O polyhedra.

The microstructures of the obtained samples were further examined with transmission electron microscopy (TEM), high-resolution transmission electron microscopy (HRTEM), and selected area electron diffraction (SAED). TEM images of 26(18)-facet Cu_2O polyhedra are shown in Figure 4a−c. Panels b and c of Figure 4 clearly display a 26-facet and 18-facet polyhedron, respectively. The dark parts indicate that two kinds of polyhedron are not a hollow structure. Figure 4d shows a HRTEM image of an 18-facet polyhedron, giving resolved lattice fringes of (001) (0.42 nm) and (110) (0.30 nm) planes. The SAED pattern (inset in Figure 4d) taken from a single polyhedron can be indexed as a cubic Cu_2O single crystal recorded along the [1−10] zone axis. TEM observations show that each particle is a single crystal.

The UV−vis absorption spectrum of as-prepared 26(18)-facet polyhedra is shown in Figure 5a. The spectral features are similar to those reported before.[13] Due to the large particle size, broad scattering bands dominate in the absorption spectrum, covering a wide range from visible light to the near-infrared region for the samples. Intrinsic band gap absorption can still be observed for the samples in the 400 to 580 nm range,[13] two broad absorption peaks at 450 and 550 nm are observed, but the bands are generally weak. Plots of $(\alpha E_{photon})^2$ versus the energy (E_{photon}) of absorbed light afford the band gap of the sample as shown in Figure 5b (where α and E_{photon} are the absorption coefficient and the discrete photon energy, respectively). The extrapolated value (the straight line to the X-axis) of E_{photon} at $\alpha = 0$ gives an absorption edge energy corresponding to $E_g = 2.13$ eV, which is in the visible light region. The evaluated band gap is near the direct band gap of 2.0−2.17 eV for bulk Cu_2O.[20,21] The UV−vis absorption spectra of Cu_2O octahedra and cubes were also measured (data not shown), and the evaluated band gap of Cu_2O octahedra and cubes is 2.34 and 2.57 eV, respectively, a little higher than that of 26(18)-facet polyhedra.

To investigate the shape effects on photocatalytic activity, Cu_2O octahedra and cubes were also prepared. From SEM images in Figure 6a,c, it can be clearly seen that Cu_2O octahedra with {111} facets exposed and cubes with {100} facets exposed have been successfully obtained. XRD patterns show that the as-prepared products are pure Cu_2O crystals (Figure 6b,d). The size of the obtained Cu_2O octahedrons and cubes is nearly the same as that of 26(18)-facet polyhedra.

Cu_2O has been used as a good visible light photocatalyst due to its narrow energy band. Photocatalytic activities of the various Cu_2O polyhedra were investigated on the decomposition of MO in aqueous solution. The orange color of the MO solution

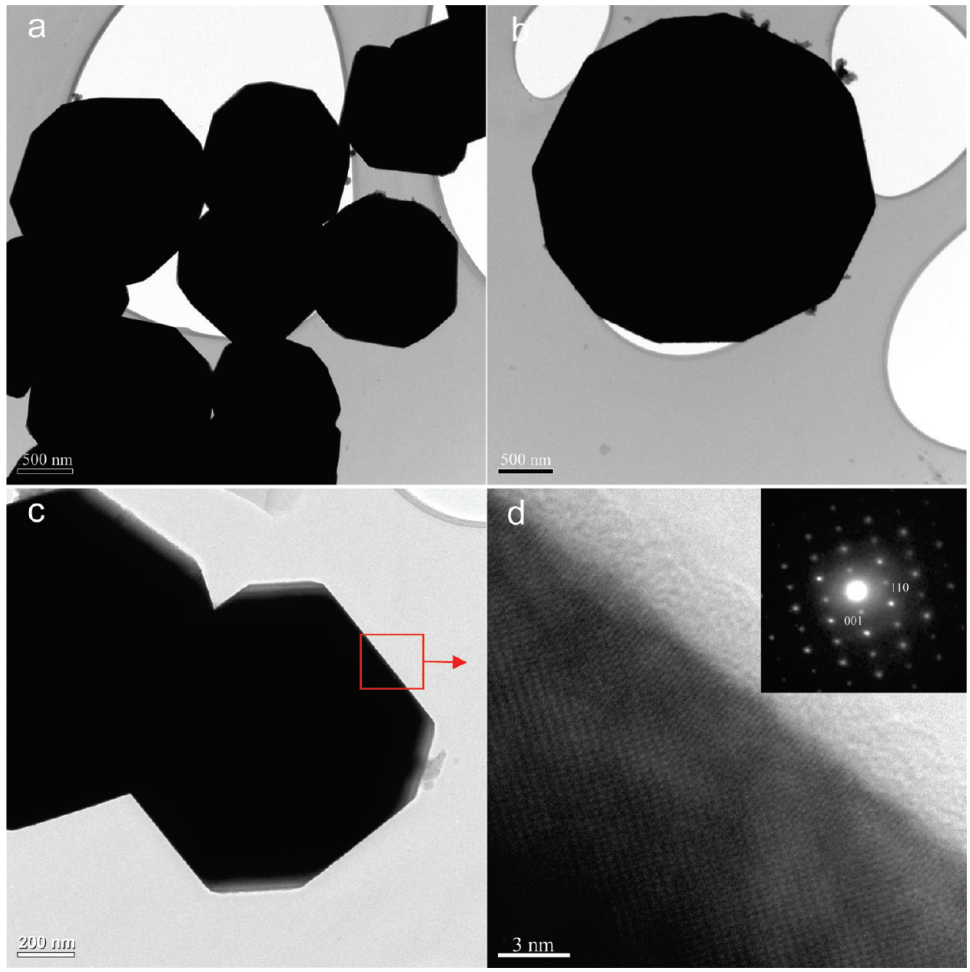

Figure 4. (a) TEM image of the 26(18)-facet polyhedra, (b) TEM image of a single 26-facet polyhedron, (c) TEM image of an 18-facet polyhedral particle, and (d) HRTEM image taken from an 18-facet polyhedral crystal (d). The inset in panel d corresponds to the SAED pattern.

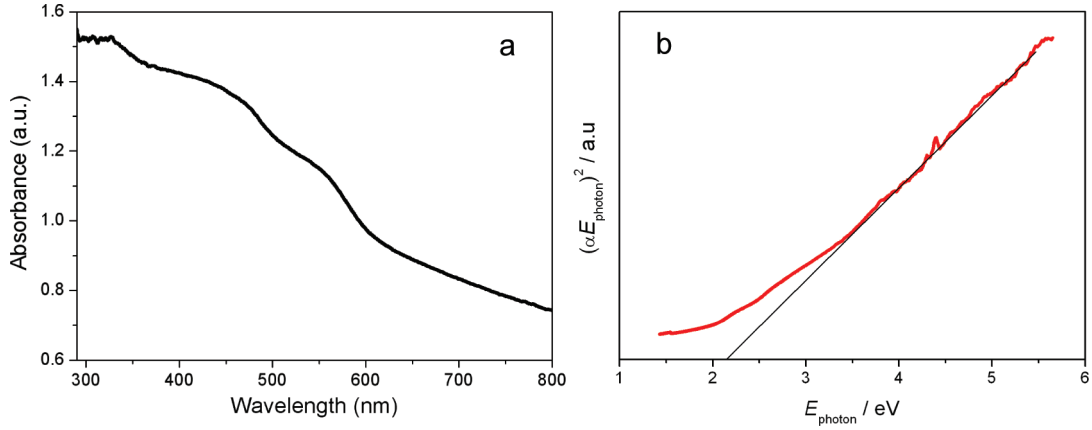

Figure 5. UV−vis absorption spectrum of Cu_2O 26(18)-facet polyhedra (a) and band gap evaluation from the plots of $(\alpha E_{photon})^2$ vs E_{photon} (b).

gradually diminished upon visible light irradiation in the presence of photocatalysts, indicating the degradation of MO. Total concentrations of MO were simply determined by the maximum absorption ($\lambda = 464$ nm) measurements. Parts a and b of Figure 6 show the absorption spectra of MO solution in the presence of Cu_2O octahedra and 26(18)-facet polyhedra at different times, from which it can be seen that the adsorption ability and photocatalytic activity of the 26(18)-facet Cu_2O particles are much higher than those of the octahedral Cu_2O particles. The results show that 26(18)-facet Cu_2O polyhedra adsorb about 73% of MO in the solution while Cu_2O octahedra adsorb about 47% for 5 h. The 26(18)-facet Cu_2O polyhedra have a much better adsorption capacity. A better photocatalytic activity of 26(18)-facet Cu_2O polyhedra than that of octahedron can be directly determined in the curve shown in Figure 7c. C/C_0 was used to describe the degradation, which stands for the concentration ratio after and before a certain reaction time. After 3 h of irradiation, the remaining MO in solution with 26(18)-facet polyhedra is 4% while it is 20% for octahedra. Obviously, the photocatalytic performance of 26(18)-facet polyhedra is better than that of octahedra.

The adsorption ability and photocatalytic activity of the octahedral Cu_2O particles is higher than those of the cubic Cu_2O particles. Octahedral Cu_2O sample degrades about 80% MO in

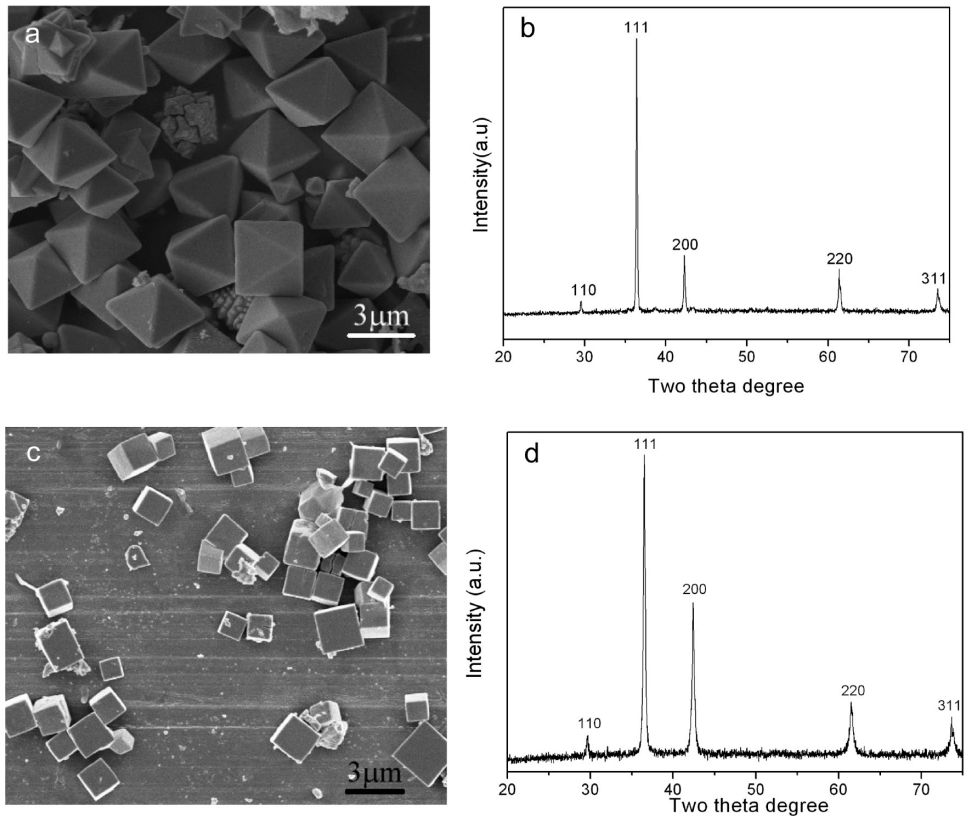

Figure 6. SEM images of Cu_2O octahedra (a) and cubes (c), and XRD patterns of Cu_2O octahedra (b) and cubes (d).

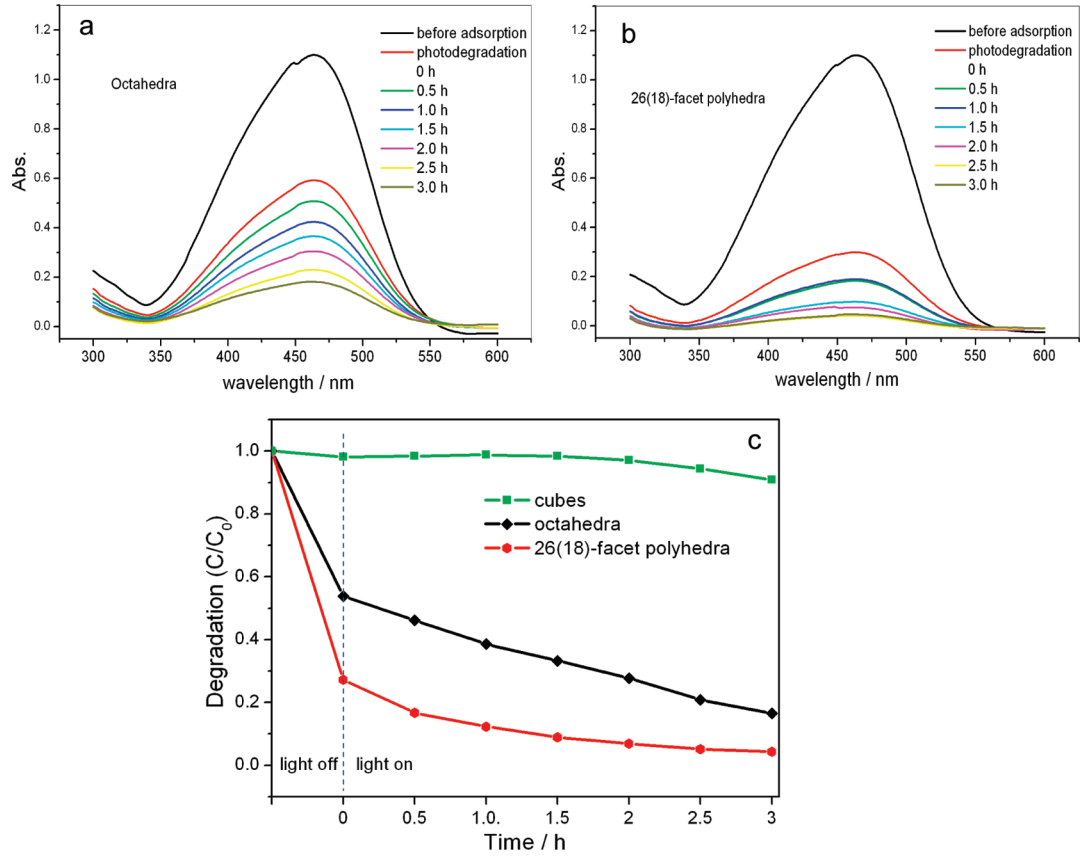

Figure 7. (a) Absorption spectra of MO solution in the presence of Cu_2O octahedra; (b) absorption spectra of MO solution in the presence of Cu_2O 26(18)-facet polyhedra; and (c) the curves of adsorption and photodegradation of MO by Cu_2O 26(18)-facet polyhedra, octahedral, and cubes, respectively.

the solution for 3 h, while cubic Cu_2O particles show ignorable either adsorption or degradation of MO (Figure 7c). This is consistent with previous studies that cubes with {100} surfaces are not active.[15,16]

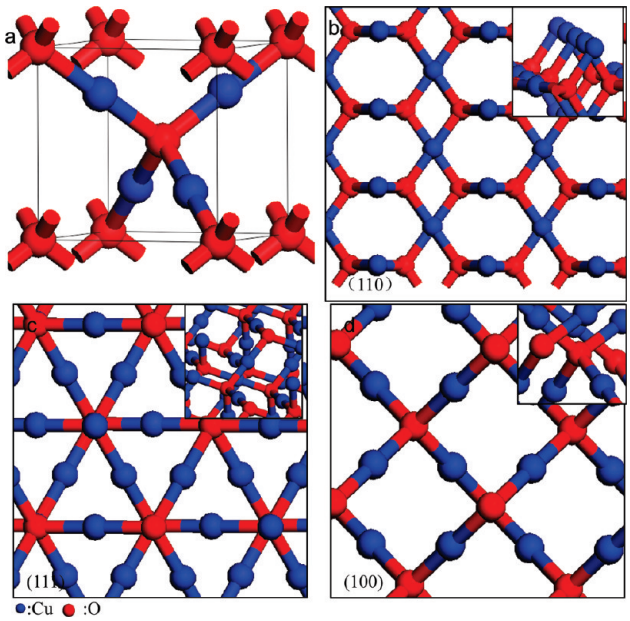

Figure 8. (a) The unit cell of the cuprous oxide Cu_2O and (b−d) the atomic arrangements in the (110) (b), (111) (c), and (100) (d) planes of the Cu_2O structure, respectively. The inset in each graph is the three-dimensional model of the terminated layer structure.

For cuprite structured Cu_2O, each "O" is surrounded by a tetrahedron of "Cu", and each "Cu" has two "O" neighbors, as displayed by its unit cell model (Figure 8a). The surface atomic arrangements of (110), (111), and (100) planes are shown in Figure 8, parts b and c, respectively, and three-dimensional models of the terminated atoms are inserted in each graph. Figure 8c shows that (111) planes with "Cu" dangling bonds are positive charged.[15] From Figure 8b it can be seen that (110) planes have the same terminated "Cu" atoms with dangling bonds, and the 3-dimensional model shows that the distance between two "Cu" atoms is about half of that in (111) planes, implying the number and a density of "Cu" dangling bonds in the (110) planes are higher than that of the (111) planes. The (100) planes have 100% saturated oxygen bonds and thus have a minimum energy state, as shown in Figure 8d.[22] Therefore, {110} and {111} facets are easily photoexited to produce electrons and holes and have better photocatalytic activity than {100} surfaces. Moreover, {110} facets of 26(18) Cu_2O polyhedra having more dangling bonds and higher surface energy show better activity than {111} facets of octahedra. Soon et al. employed the technique of "*ab initio* atomistic thermodynamics" to identify the surface structures of the (110) and (111) planes, and found that both of them exhibit a metallic character, but their electronic structures are rather different. The (111) plane structure's metallic character is largely bulk-like in nature, whereas that of the (110) plane structure is truly surface-like, which may result in better catalytic activity related to the "Cu" dangling bonds of the {110} surfaces.[23] Additionally, the positively charged {110} and {111} facets should interact more strongly with negatively charged MO molecules than the electrically neutralized {100} facet does, which offers the 26(18)-facet Cu_2O polyhedra and the octahedral Cu_2O particles a higher adsorption ability than the cubic Cu_2O particles.

On the other hand, as compared with octahedra, 26(18)-facet Cu_2O polyhedra have more edges and corners which could improve the photocatalytic activity, as demonstrated in previous studies on other materials.[1,2]

The data clearly imply that exposure of a greater proportion of polar faces leads to higher photocatalytic activity. The better activity of the {110} surfaces could be attributed to the intrinsically highest energy among all the faces. The OH^- ions could preferentially adsorb onto this face because of its positive charge. This would lead to a greater rate of production of $OH^\bullet$ radicals, and hence degradation of the dye, during the photocatalytic reaction.[24] An alternative insight into high activity in the (110) faces could be that there is a positive correlation between the proportion of polar (110) faces exposed and the surface oxygen vacancy content of samples, as reported for ZnO photocatalyst.[25] Oxygen vacancies in Cu_2O undoubtedly can act as potential wells to trap either one or two electrons, helping electron−hole pair separation and hence increasing the photocatalytic activity. It was previously reported that exposure of a greater proportion of polar faces such as (001) faces of ZnO and (001) faces of TiO_2 led to greater photocatalytic activity.[24,26] Further study is therefore needed in order to explore the origin of the high photocatalytic activity of the {110} facets of Cu_2O polyhedra found in this work.

Conclusions

In summary, we have successfully synthesized perfect mixed 26-facet and 18-facet polyhedra of Cu_2O microcrystals by taking advantage of the selective surface stabilization of stearic acid on {110} facets of Cu_2O by hydrothermal treatment. The polyhedral structures were characterized by XRD pattern, TEM measurements, and UV−vis spectrum analysis in detail. By changing the reaction conditions, Cu_2O octahedra and cubes were also produced. Methyl orange was chosen to be photodegraded in aqueous solution using as-prepared 26-facet and 18-facet Cu_2O polyhedra, octahedra, and cubes. The as-prepared Cu_2O polyhedra exhibited a facet-related adsorption and photocatalytic activity to MO. Due to the specific structure of 26-facet and 18-facet Cu_2O polyhedra, they show a higher adsorption and better photodegradation ability than octahedra and cubes. This finding further implies that the performance of catalysts can be enhanced by shape control as shape determines the number of atoms located at the edges, corners, or surfaces. Our study could promote the synthesis of other materials and the applications of polyhedra with active surfaces in the catalytic field.

Acknowledgment. Support from the National Natural Science Foundation of China (20971118, 20901081), the 100 Talents program of the Chinese Academy of Sciences, and Anhui Natural Science Foundation Key Project (ZD200902) is gratefully acknowledged.

References and Notes

(1) Narayanan, R.; El-Sayed, M. A. *J. Phys. Chem. B* **2005**, *109*, 12663.
(2) Xiong, Y. J.; Wiley, B. J.; Xia, Y. N. *Angew. Chem., Int. Ed.* **2007**, *46*, 7157.
(3) (a) Zecchina, A.; Groppo, E.; Bordiga, S. *Chem.—Eur. J.* **2007**, *13*, 2440. (b) Bratlie, K. M.; Lee, H.; Komvopoulos, K.; Yang, P. D.; Somorjai, G. A. *Nano Lett.* **2007**, *7*, 3097.
(4) Yang, H. G.; Liu, G.; Qiao, S. Z.; Sun, C. H.; Jin, Y. G.; Smith, S. C.; Zou, J.; Cheng, H. M.; Lu, G. Q. *J. Am. Chem. Soc.* **2009**, *131*, 4078.
(5) Tian, N.; Zou, Z. Y.; Sun, S. G.; Ding, Y.; Wang, Z. L. *Science* **2007**, *316*, 732.
(6) (a) Kim, F.; Connor, S.; Song, H.; Kuykendall, T.; Yang, P. D. *Angew. Chem., Int. Ed.* **2004**, *43*, 3673. (b) Sun, Y. G.; Xia, Y. N. *Science* **2002**, *298*, 2176.
(7) (a) Hao, Y. F.; Meng, G. W.; Ye, C. H.; Zhang, L. D. *Cryst. Growth Des.* **2005**, *5*, 1617. (b) Shi, M. R.; Xu, F.; Yu, K.; Zhu, Z. Q.; Fang, J. H. *J. Phys. Chem. C* **2007**, *111*, 16267. (c) Yang, H. G.; Zeng, H. C. *Angew. Chem., Int. Ed.* **2004**, *43*, 5930.
(8) Cao, H. L.; Qian, X. F.; Wang, C.; Ma, X. D.; Yin, J.; Zhu, Z. K. *J. Am. Chem. Soc.* **2005**, *127*, 16024.

(9) (a) Poizot, P.; Laruelle, S.; Grugeon, S.; Dupont, L.; Taracon, J. M. *Nature* **2000**, *407*, 496. (b) Liu, R.; Kulp, E. A.; Oba, F. E.; Bohannan, W.; Ernst, F.; Switzer, J. A. *Chem. Mater.* **2005**, *17*, 725.

(10) (a) Xiong, Y. J.; Li, Z. Q.; Zhang, R.; Xie, Y.; Yang, J.; Wu, C. Z. *J. Phys. Chem. B* **2003**, *107*, 3697. (b) Wang, W. Z.; Wang, G. H.; Wang, X. S.; Zhan, Y. J.; Liu, Y. K.; Zheng, C. L. *Adv. Mater.* **2002**, *14*, 67.

(11) Chang, Y.; Zeng, H. C. *Cryst. Growth Des.* **2004**, *4*, 273.

(12) (a) Gou, L. F.; Murphy, C. J. *Nano Lett.* **2003**, *3*, 231. (b) Siegfried, M. J.; Choi, K. S. *Adv. Mater.* **2004**, *16*, 1743. (c) Siegfried, M. J.; Choi, K. S. *Angew. Chem., Int. Ed.* **2005**, *44*, 3218.

(13) (a) Lu, C. H.; Qi, L. M.; Yang, J. H.; Wang, X. Y.; Zhang, D. Y.; Xie, J. L.; Ma, J. M. *Adv. Mater.* **2005**, *17*, 2562. (b) Guo, S. J.; Fang, Y. X.; Dong, S. J.; Wang, E. K. *Inorg. Chem.* **2007**, *46*, 9537. (c) Kou, C. H.; Huang, M. H. *J. Am. Chem. Soc.* **2008**, *130*, 12815.

(14) Zhang, D. F.; Zhang, H.; Guo, L.; Zheng, K.; Han, X. D.; Zhang, Z. *J. Mater. Chem.* **2009**, *19*, 5220.

(15) Ho, J. Y.; Huang, M. H. *J. Phys. Chem. C* **2009**, *10*, 1021.

(16) Xu, H. L.; Wang, W. Z.; Zhu, W. *J. Phys. Chem. B* **2006**, *110*, 13829.

(17) Song, R. Q.; Xu, A. W.; Antonietti, M.; Cölfen, H. *Angew. Chem., Int. Ed.* **2009**, *48*, 395.

(18) (a) Sun, X.; Zhang, Y. W.; Si, R. W.; Yan, C. H. *Small* **2005**, *1*, 1081. (b) Xu, J. S.; Xue, D. F. *Acta Mater.* **2007**, *55*, 2397.

(19) (a) Wang, Z. L. *J. Phys. Chem. B* **2000**, *104*, 1153. (b) Wiley, B.; Sun, Y.; Mayers, B.; Xia, Y. *Chem.—Eur. J.* **2005**, *11*, 454.

(20) Snoke, D. *Science* **1996**, *273*, 1351.

(21) Ng, C. H. B.; Fan, W. Y. *J. Phys. Chem. B* **2006**, *110*, 20801.

(22) Le, D.; Stolbov, S.; Rahman, T. S. *Surf. Sci.* **2009**, *603*, 1637.

(23) Soon, A.; Todorova, M.; Delley, B.; Stampfl, C. *Phys. Rev. B* **2007**, *75*, 125420.

(24) Mclaren, A.; Valdes-Solis, T.; Li, G. Q.; Tsang, S. C. *J. Am. Chem. Soc.* **2009**, *131*, 12540.

(25) Li, G. R.; Hu, T.; Pan, G. L.; Yan, T. Y.; Gao, X. P.; Zhu, H. Y. *J. Phys. Chem. C* **2008**, *112*, 11859.

(26) Zhang, D. Q.; Li, G. S.; Yang, X. F.; Yu, J. C. *Chem. Commun.* **2009**, 4381.

JP9110037